Supporting Information

Jacobson *et al*. 10.1073/pnas.0806661106

SI Text

Frequency Changes Are Related to the Behavioral State of the Rat. The epochs of frequency elevation observed in the oscillatory activity were intermittent in nature and lasted several seconds. To study whether these epochs were related to rat behavior, rat behavior was monitored by using a single video camera at 30 frames/s ($n = 4$ rats). Movies were then manually analyzed, and segmented into epochs during which the rat was still and moving. Tremor was not quantitatively monitored, but was observed in all rats and appeared enhanced during volitional movement. After harmaline application, rats spent 19–45% of the time moving around the cage. During movement epochs, changes could be observed in the spectrograms of the MUA (Fig. S2*a*) (yellow bars denote epochs). Movement was associated with an average shift of 6.7% in the frequency peak (examples in Fig. S2*b*). All experiments analyzed for movement exhibited shifts in the 6.7–20% range (Fig. S2*c*). Covert changes in the arousal state of the rat, or other behavioral parameters, may more fully account for the frequency variability. These results imply that marked global changes in oscillation frequency are correlated with changes in the behavioral state of the animal.

The Relationship Between Phase Maintenance and Delay Maintenance. We have shown (Fig. 4) that the phase difference between electrode pairs is well maintained, although time delays are not. How are these two measures related to each other? Assume that the oscillatory activity switches between 2 discrete values, F_1 and F_2 ($F_1 < F_2$). Under the assumption of phase constancy, we can attribute a phase difference value to some electrode pair, denoted as $\Delta\varphi$ (assume $\Delta\varphi \neq 0$, as this case has trivial zero phase and delay). This phase difference corresponds to different delays in the 2 frequency regimes:

$$\Delta t_1 = \frac{1}{F_1} \cdot \frac{\Delta\varphi}{2\pi}$$

$$\Delta t_2 = \frac{1}{F_2} \cdot \frac{\Delta\varphi}{2\pi}$$

Phase constancy therefore implies that the delay/delay graph depicted in Fig. 4*D* should have a slope of

$$\frac{\Delta t_2}{\Delta t_1} = \frac{F_1}{F_2} < 1$$

as seen in the results. The exact delay/delay slope value depends on the percent frequency change between the 2 discrete frequency values. Noninvariance of the delay does therefore not imply that delay values in the 2 frequency ranges are uncorrelated, but rather determines a certain slope value <1. In a similar fashion, delay invariance would have led to phase/phase slope values >1, a phenomenon never observed in the data.

Anatomical Location of Recording Electrodes. Microelectrode arrays were chronically implanted in the depth of vermal lobule V/VI (0.8–2 mm). Electrode position within the cerebellar cortex was verified histologically. In brief, electrical lesions were done under anesthesia by passing an electrical current (10 μA, 8–15 s) (Stoelting) between recording electrodes and a ground connected to the screws passing through the rat skull. Animals were kept under anesthesia for ≈1 h, and euthanized (pentobarbital, i.p.). Saline (NaCl, 0.9%, ≈200 ml) was initially perfused through the heart at a rate of 10 ml/min. by using a peristaltic pump (MasterFlex), and then perfusion was switched to formaldehyde (4%) in PBS (≈500 ml, same perfusion rate). The brain was then carefully removed and kept in formaldehyde-PBS solution for 2 days. Para-sagittal slices (75-μm thick) were cut by using a vibratome and stained with haemotoxylin. Electrode tracks (arrow in Fig. S3*a*) and lesion sites could be observed on different slices and different cortical layers (* in Fig. S3 *a* and *b*). In Fig. S3*a*, the lesion is in the PC layer, whereas in Fig. S3*b*, 3 lesions are observed, 2 in the PC/molecular layer, and 1 in the white matter. The minority of electrodes that did not detect harmaline-induced oscillatory activity were probably located in the granule cell/white-matter layers.

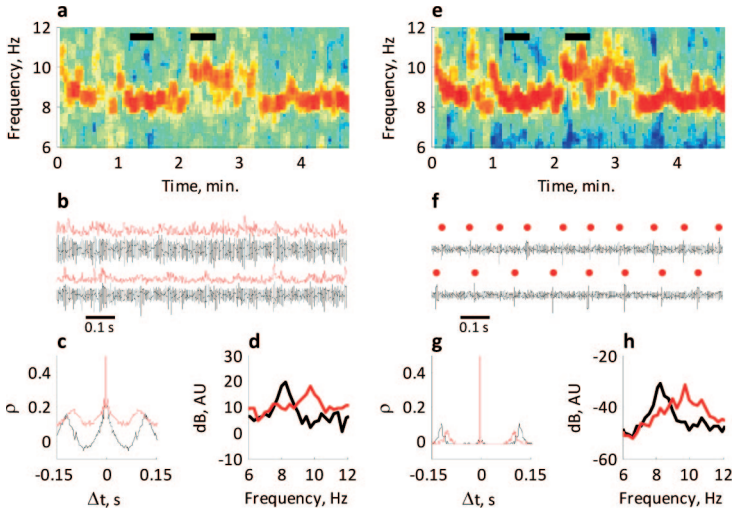

Fig. S1. Single-unit-complex spikes exhibit episodes of frequency elevation simultaneously with the multiunit activity envelopes. (*a*) Spectrogram of MUA envelope segment, demonstrating a long epoch of frequency elevation. Black bars mark 40-s segments of baseline (*Left*, ≈8.5 Hz) and elevated (*Right*, ≈9.7 Hz) frequency analyzed in *b*–*d*. (*b*) Segments of (1 s) of raw-voltage trace (black) and envelope (red) during baseline (below) and elevated (above) frequency are shown. (*c*) Autocorrelation of envelope during baseline (black, left black bar in *a*) and elevated (red, right black bar in *a*) frequency. (*d*) Power spectrum of the envelopes in the 2 frequency ranges. (*e*) Spectrogram of single-unit-CS activity, taken from a different electrode, simultaneously recorded with the electrode in *a*–*d*. (*f*–*h*) Same frequency analysis as *b*–*d* for the single-unit CS data.

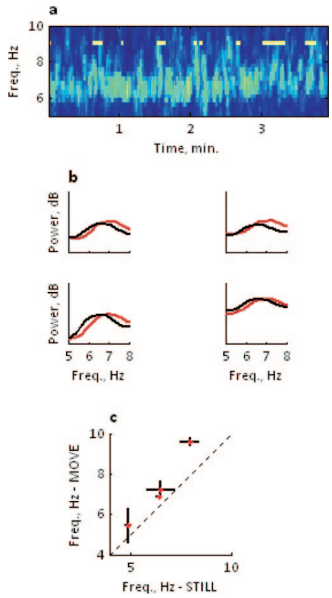

Fig. S2. Frequency changes are related to the arousal state of the rat. (*a*) Spectrogram of envelope fluctuations, with arousal periods (animal movement) marked by yellow bars. (*b*) Power spectrum of envelope fluctuations on 4 different electrodes, averaged across rest (black) and movement (red), demonstrates the 6.7% frequency elevation observed in this experiment. (*c*) Mean ± 1 SD of peak oscillation frequency while the animal was still (abscissa) and moving (ordinate) for all taped experiments ($n = 4$).

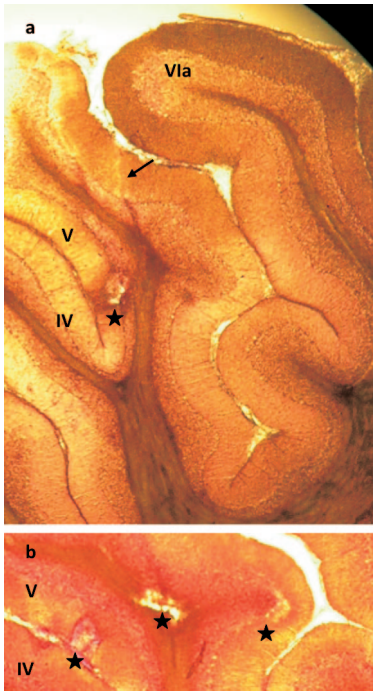

Fig. S3. Location of electrodes in cerebellum. (*a*) Para-sagittal slice through cerebellar vermis shows the location of 1 electrode track (arrow) and lesion site (*). (*b*) A second slice, ≈1.5 μm lateral to the one in *a*, shows 3 clear lesions, 2 of them in the PC layer/molecular layer of lobule V.

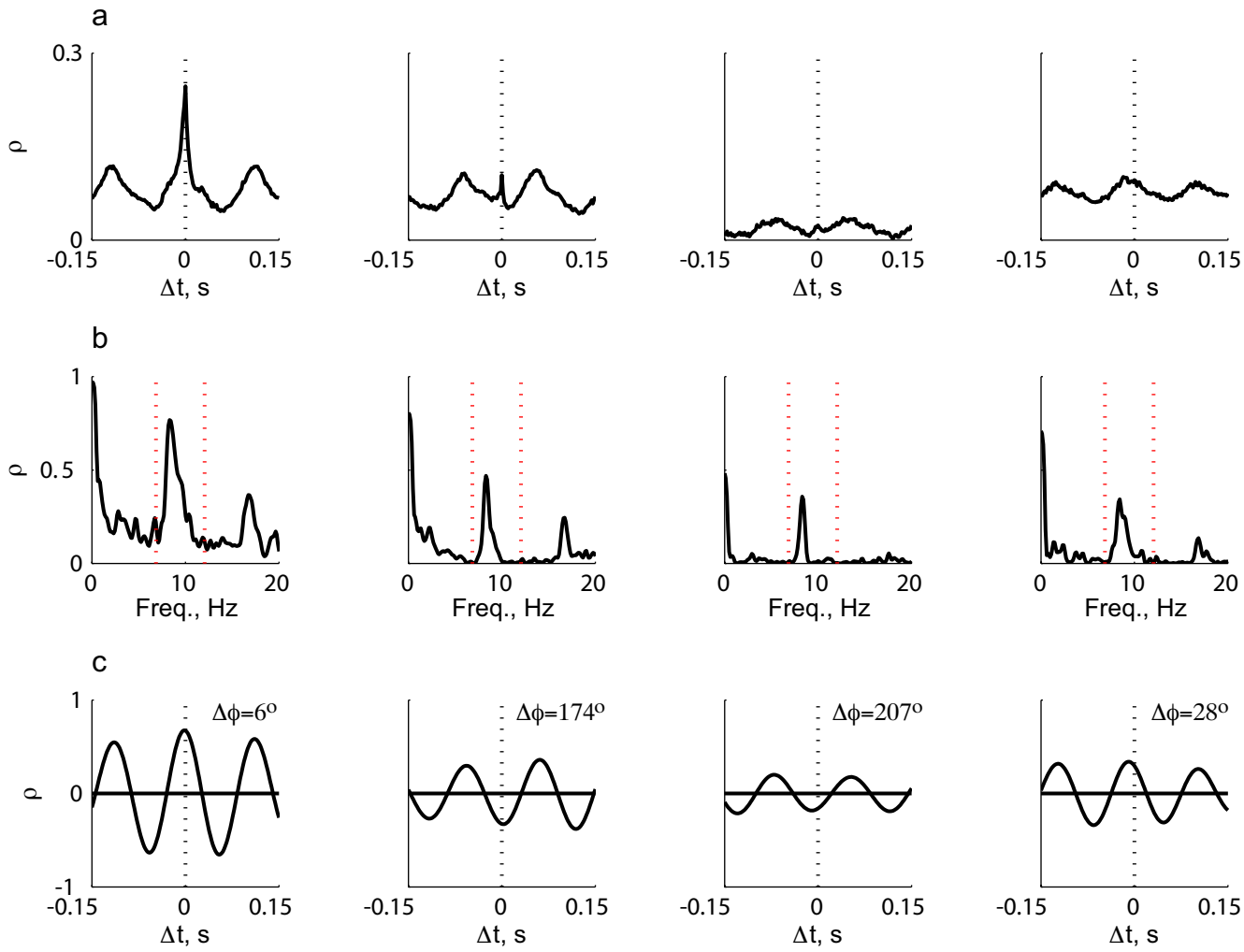

Fig. S4. Method used to create narrow-band envelope signals and for extracting relative phase. (*a*) Cross correlations from 4 electrode pairs recorded simultaneously, exhibiting a variety of correlation strengths and correlation phases. (*b*) Coherence between the envelope pairs in *a*. Vertical red lines demarcate the frequency band used for extracting narrow-band envelopes (similar for all electrodes). (*c*) Cross-correlations from the 4 electrode pairs in *a*, performed on the narrow-band-envelope signals. The narrow-band property allows the extraction of relative phase ($\Delta\phi$) from each pair.